ELSEVIER

European Journal of Radiology 65 (2008) 228–234

EJR
EUROPEAN JOURNAL OF RADIOLOGY

www.elsevier.com/locate/ejrad

Quantitative analysis of emphysema in 3D using MDCT: Influence of different reconstruction algorithms

Julia Ley-Zaporozhan [a,b,*,1], Sebastian Ley [b,c,1], Oliver Weinheimer [a], Svitlana Iliyushenko [b], Serap Erdugan [b], Ralf Eberhardt [d], Adelheid Fuxa [b], Jürgen Mews [e], Hans-Ulrich Kauczor [b]

[a] *Department of Radiology, Johannes Gutenberg University Hospital, Langenbeckstr. 1, 55131 Mainz, Germany*
[b] *Department of Radiology (E-010), German Cancer Research Center, Im Neuenheimer Feld 280, 69120 Heidelberg, Germany*
[c] *Department of Pediatric Radiology, Ruprecht-Karls-University, Heidelberg, Germany*
[d] *Department of Pulmology, Thoraxklinik, Heidelberg, Germany*
[e] *Toshiba Medical Systems, Germany*

Received 2 October 2006; accepted 28 March 2007

Abstract

Purpose: The aim of the study was to compare the influence of different reconstruction algorithms on quantitative emphysema analysis in patients with severe emphysema.

Material and methods: Twenty-five patients suffering from severe emphysema were included in the study. All patients underwent inspiratory MDCT (Aquilion-16, slice thickness 1/0.8 mm). The raw data were reconstructed using six different algorithms: bone kernel with beam hardening correction (BHC), soft tissue kernel with BHC; standard soft tissue kernel, smooth soft tissue kernel (internal reference standard), standard lung kernel, and high-convolution kernel. The only difference between image data sets was the algorithm employed to reconstruct the raw data, no additional radiation was required. CT data were analysed using self-written emphysema detection and quantification software providing lung volume, emphysema volume (EV), emphysema index (EI) and mean lung density (MLD).

Results: The use of kernels with BHC led to a significant decrease in MLD (5%) and EI (61–79%) in comparison with kernels without BHC. The absolute difference (from smooth soft tissue kernel) in MLD ranged from −0.6 to −6.1 HU and were significant different for all kernels. The EV showed absolute differences between −0.05 and −0.4 L and was significantly different for all kernels. The EI showed absolute differences between −0.8 and −5.1 and was significantly different for all kernels.

Conclusion: The use of kernels with BHC led to a significant decrease in MLD and EI. The absolute differences between different kernels without BHC were small but they were larger than the known interscan variation in patients. Thus, for follow-up examinations the same reconstruction algorithm has to be used and use of BHC has to be avoided.

Keywords: Lung; Emphysema: Computed tomography; Emphysema detection software; Reconstruction algorithm; Pulmonary function tests

1. Introduction

High resolution CT (HRCT) is an established and well accepted method for non-invasive characterisation of emphysema [1]. State-of-the-art multi-detector CT imaging (MDCT) allows acquisition of the whole lung in thin sections of 1 mm. These high resolution 3D datasets (HR-MDCT) are mandatory to distinguish parenchymal alterations exhibited in emphysema and to assess regional variations [2]. HR-MDCT can characterize anatomic details of the lung as small as 200–300 μm, which correspond to approximately the seventh to ninth generations of airways and lung segments [2].

Low attenuation areas on CT represent macroscopic and microscopic emphysematous changes of the lung [3]. Objective quantification of emphysema can be obtained by measuring the relative lung area occupied by pixels with attenuation

* Corresponding author at: Department of Radiology, Johannes Gutenberg University Hospital, Langenbeckstr. 1, 55131 Mainz, Germany. Tel.: +49 1775141849.
E-mail address: juliazapo@web.de (J. Ley-Zaporozhan).

[1] These authors have contributed equally.

0720-048X/$ – see front matter © 2007 Elsevier Ireland Ltd. All rights reserved.
doi:10.1016/j.ejrad.2007.03.034

coefficients below a predetermined threshold [4–6]. Quantitative evaluation of emphysema will be a key feature for serial follow-up examinations of patients with chronic obstructive pulmonary disease (COPD). Especially, as new treatment options for emphysema become available (e.g. phosphodiesterases inibitors) [7,8].

The 3D nature of HR-MDCT datasets allow excellent quantitative evaluation of whole lung in emphysema which is important as emphysema has a heterogeneous distribution [9]. Established parameters in quantitative CT data are mean lung density (MLD) and emphysema index (EI) [4,10]. Quantitative analysis has been transferred to 3D HR-MDCT [11]. In 3D, it is also possible to calculate lung volumes (LV) and emphysema volumes (EV).

Besides patient size and lung volume, technical parameters, such as slice thickness, kV, and mA s can affect comparability of quantitative information [12,13]. When CT scan data are reconstructed with different algorithms, the mean Hounsfield unit (HU) value of a region is expected to stay the same, but the distribution of attenuation values and thus measures derived from this distribution might change. A recently published study demonstrated that the selection of the reconstruction algorithm, especially overenhancing algorithms, may strongly affect density mask results from CT lung images in patients with emphysema [13]. However, this was only demonstrated on 10 mm thick slices which must not be used for the quantification of emphysema [14,15].

Large HU differences as seen at air or soft tissue to bone interfaces lead to beam hardening artefacts. This can be the case in the paravertebral regions. Dedicated reconstruction kernels were developed to reduce those artefacts (beam hardening correction, BHC) [16]. However, the effect of BHC on quantitative evaluation was not yet demonstrated.

Thus, the aim of our study was to reconstruct 3D HR-MDCT datasets of a phantom and patients with emphysema with different reconstruction algorithms. The effect on quantitative evaluation of emphysema was done using an advanced dedicated semiautomatic analysis tool. To demonstrate clinical impact of the results they were correlated with pulmonary function test (PFT).

2. Materials and methods

2.1. Computed tomography

CT was performed using a 16-row-MDCT (Aquilion-16, Toshiba, Japan). The CT parameters for all acquisitions were: collimation 1 mm, 120 kV, 150 mA s, gantry rotation time 0.5 s and pitch 1.5, large scan field. All images were reconstructed with a slice thickness 1 mm and reconstruction interval of 0.8 mm.

The raw image data were reconstructed at the scanner with six different reconstruction algorithms (Toshiba code): two kernels with beam hardening correction (BHC)—bone kernel (FC 03) and soft tissue kernel (FC 69); four kernels without beam hardening—standard soft tissue kernel (FC 10), smooth soft tissue kernel (FC 12), standard lung kernel (FC 51), and high-convolution kernel (FC 85). It is important to emphasize that the only difference between image data sets was the algorithm employed to reconstruct the raw data, and thus no additional radiation was required to produce these additional data sets.

2.2. Phantom

We scanned a large field water phantom with the same technical parameters and reconstructed the data using six different kernels. At identical image positions five slices were evaluated for each kernel using a ROI analysis ($d = 400$ mm, i.e. whole field of view), resulting in mean, median, maximum (max) and minimum (min) values and standard deviation (S.D.).

2.3. Patients

Twenty-five consecutive patients (7 females and 18 males; mean age 60 ± 8 years, range 41–74) were included in this study. All patients were suffering from severe emphysema (on CT scans severe emphysema was present).

The study was approved by the local ethics committee. All subjects were informed prior to the investigation. The CT examination was performed as part of routine standard work-up of the patients for tentative surgical [17] or endobronchial treatment [18,19]. Inclusion criteria for the tentative treatment were smoking history, severe changes in lung function tests indicative for obstructive disease and exclusion of α_1-antitrypsin deficiency.

CT was done during inspiratory breath-hold in supine position. The breath-hold period was 10–13 s depending on the individual lung size. For thoracic coverage, 311–509 (mean 422 ± 37) images were reconstructed. No intravenous contrast medium was administered.

2.3.1. Pulmonary function test

All patients had PFT performed on a bodyplethysmograph (MasterScreen® Body, Jaeger, Germany) according to the guidelines of the European Respiratory Society [20]. The following volume measurements were chosen for correlation: total lung capacity (TLC), intrathoracic gas volume (ITGV) and residual volume (RV). Furthermore, the transfer factor for carbon monoxide% predicted (TL_{CO}% predicted) was determined.

2.3.2. Image analysis

All patient images were transferred via routine PACS to a PC (Intel Pentium 4, 2.7 GHz, 768 MB RAM, Windows XP Prof.), where a self-written software (YACTA®, Mainz, Germany) was used for evaluation. As the principle of the software was described in detail in other studies, here only a condensed description is included, focusing on the most important points [21–23]. The software combines different techniques for semi-automatic segmentation of the lungs like region growing, threshold- and expert-based methods, and morphological analysis. A denoising filter was applied to all images reconstructed using lung kernel because of too much noise for the software evaluation. All other algorithms were evaluated without a denoising filter. Important morphological thoracic landmarks, i.e. trachea, right, and left lung, were automatically detected. The trachea and the bronchi up to the eighth generation were automatically segmented and excluded from emphysema evaluation as they contain "dead respiratory space".

On the basis of the pulmonary landmarks, the lung is detected by a region growing with a N6 neighbourhood system and an upper threshold of −500 HU. All voxels marked as lung parenchyma were analysed. Voxels below -950 HU were segmented as emphysema [14,15,24]. This was followed by a correction factor which included all voxels from −950 to −910 HU if they were completely surrounded by emphysema voxels.

From this analysis, we received the total lung volume (LV), emphysema volume (EV), emphysema index (EI), and mean lung density (MLD) for the whole lung.

The software was applied to all CT-datasets. The results were correlated to the parameters of PFT as described above. Data analysis was done using Microsoft Excel 2003 SP 2. For correlation between different results linear regression analysis was comprised. Origin® (Version 6.1G, OriginLab Corporation, USA) was used for the box-plot diagrams.

Testing for interkernel differences the Wilcoxon-Signed-Rank test was used (SPSS for Windows, Version 12). A p-value < 0.05 was assumed to be significant different.

3. Results

3.1. Phantom

The results for the water phantom are given in Fig. 1. The FC 51 and FC 85 kernels showed a broad spectrum of HU values (huge difference of min and max) and with a high S.D. All kernels showed mean and median values for water in the normal range.

As FC 12 showed the lowest standard variation (52 HU) and min/max values (−239/233 HU), the quantitative results of this kernel were used as internal reference standard. Results of all other kernel were tested for difference to FC 12.

The mean HU of FC 03 and FC 69 showed significant differences compared to FC 12 (p = 0.03 and 0.04, respectively). The other kernels showed no significant differences (FC 10: p = 0.4; FC 51: p = 1; FC 85: p = 0.3).

3.2. Kernels with BHC (FC 03 and FC 69)

Applying the same kernels to the first five emphysema patients the results for the EV showed a broad range of 0.9 L for FC 03, 1.8 L for FC 69, and 5.1–5.2 L for the other kernels (Fig. 2; Table 1).

The same was found for the EI, where the difference between FC 12 and FC 03 was 47% and FC 69 was 37%. Only small differences were found for FC 10 (−1%), FC 51 (0%), and FC 85 (−5%). However, FC 03, FC 69, FC 10, and FC 85 were significantly different (p = 0.04) compared to FC 12. Only FC 51 (with gauss filter applied) showed no difference (p = 0.9).

Based on these evaluations the kernel FC 03 and FC 69 were excluded from further analysis.

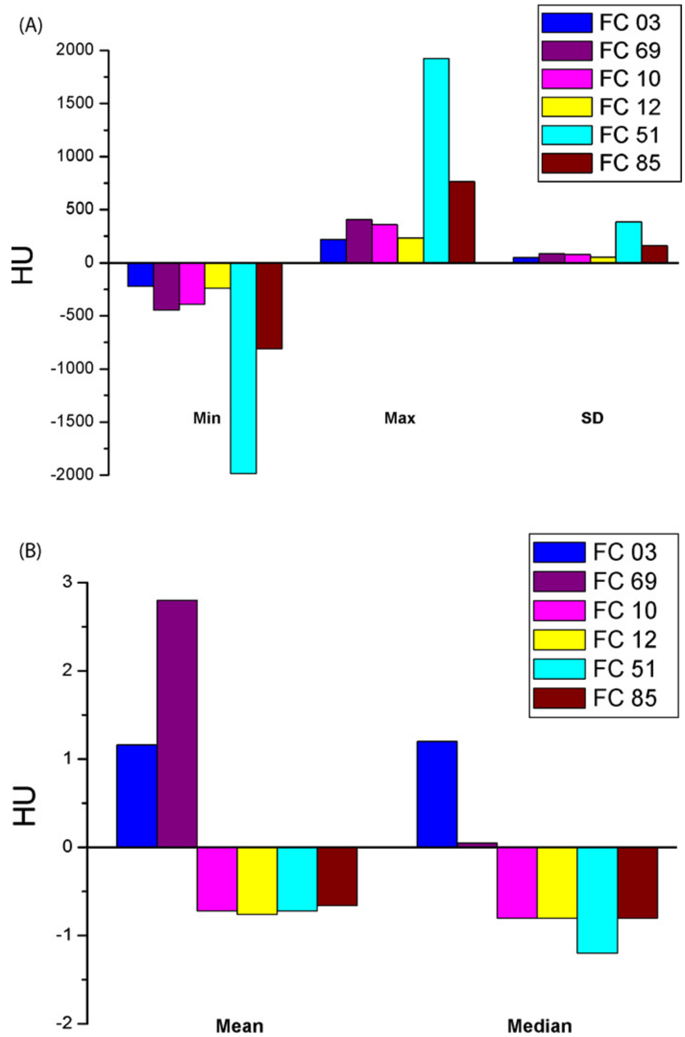

Fig. 1. Results for the phantom measurements showing the standard deviation (S.D.), minimal, and maximal values (A) and mean and median values (B) for all kernels. The evaluation was performed without use of any denoising filter. FC 51 and FC 85 present the highest minimum and maximum values and the highest standard deviation. All kernels showed mean and median values for water in the normal range.

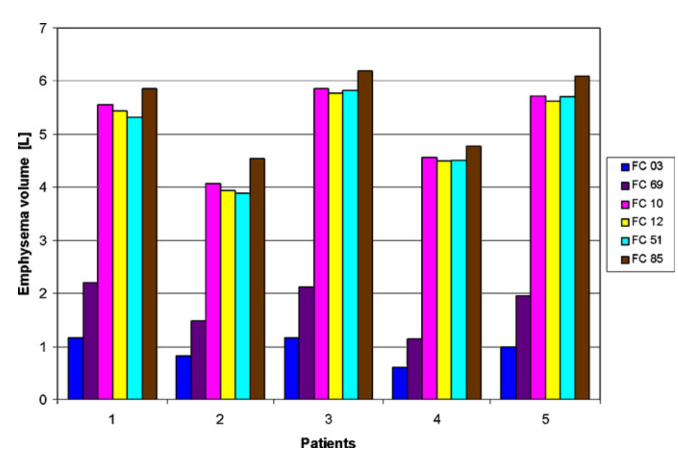

Fig. 2. Results for the emphysema volumes in five patients for all kernels. There were large differences between those kernels with beam hardening correction (BHC) (FC 03 and FC 69) to those without BHC (FC 10, 12, 51, and 85).

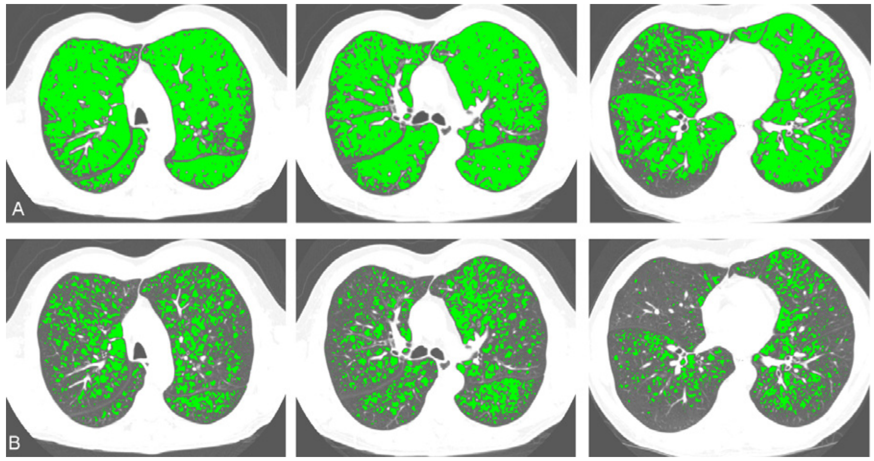

Fig. 3. Axial CT images of the same patients reconstructing using (A) smooth soft tissue kernel (FC 12) and (B) soft tissue kernel with BHC (FC 69). The emphysema voxels are coloured in green. The detected emphysema volume was 5.6 L for FC 12 and 2 L for FC 69.

Table 1
These tables summarize the quantitative results (mean) of all parameters evaluated in five patients using all kernels

Kernels	Lung volume (L)	Emphysema volume (L)	Emphysema index (%)	MLD (HU)
FC 03	8.2	0.9	12.7	−853.8
FC 69	8.3	1.8	23.2	−855.2
FC 10	8.4	5.2	61.1	−902.4
FC 12	8.4	5.1	59.8	−903.4
FC 51	8.4	5.1	59.9	−897
FC 85	8.4	5.5	65.1	−902.8

Fig. 3 presents the difference in detection of EV dependent on the kernel.

3.3. Kernels without BHC

The remaining four kernels were analysed for LV, MLD, EV, and EI in all 25 patients. The detailed results are presented in (Table 2). No significant difference was found for the LV for kernels FC 10 and FC 51 ($p > 0.2$) and a significant difference for FC 85 ($p = 0.002$). The absolute difference in MLD (from FC 12) ranged from −0.6 to −6.1 HU and were significant different for all kernels. The EV showed absolute differences between −0.05 and −0.4 L and was significantly different for all kernels (Fig. 4).

The EI was significantly different for all kernels (compared to FC 12) with $p < 0.001$ (FC 10 and FC 85) and $p = 0.01$ (FC 51) (Table 3). However, the absolute differences for EI were only −1.4 ± 0.5% (FC 10), −0.8 ± 1.4% (FC 51), and −5.1 ± 2.0% (FC 85).

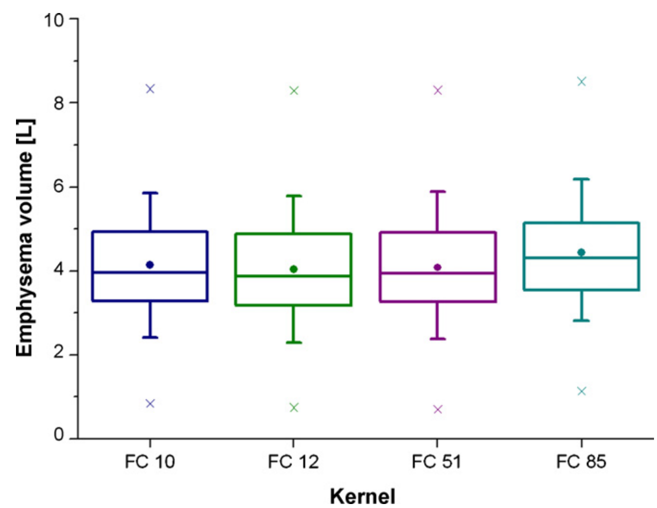

Fig. 4. Box-plot diagrams of the emphysema volume quantified in CT using different kernels: 25–75% range ( ), 5–95% range ( ), mean (●), median ( ), minimum and maximum (✖).

3.4. Correlation with PFT

TLC derived form PFT revealed a strong linear correlation with LV (all kernels, $R = 0.86$). The EV showed a strong correlation with ITGV ($R = 0.83$–0.85) and RV ($R = 0.81$–0.82)

Table 2
This table summarizes the CT results for 25 patients in for quantitative parameters

Kernels	Lung volume (L)	Emphysema volume (L)	Emphysema index (%)	MLD (HU)
FC 10	7.28 ± 1.32 (0.7)	4.13 ± 1.49 (0.001)	55.4 ± 12.6 (0.001)	−895.2 ± 22.6 (<0.001)
FC 12	7.28 ± 1.32 (–)	4.04 ± 1.5 (–)	54 ± 12.9 (–)	−896.1 ± 22.6 (–)
FC 51	7.27 ± 1.31 (0.2)	4.09 ± 1.5 (0.01)	54.8 ± 13.1 (0.01)	−890 ± 22.7 (<0.001)
FC 85	7.27 ± 1.32 (0.002)	4.45 ± 1.46 (0.001)	59.9 ± 11.5 (0.001)	−895.5 ± 22.7 (0.001)

Data are given as mean ± standard deviation (p-value tested against FC 12).

Table 3
This table gives the detailed description of the emphysema index for all 25 patients with the minimum and maximum of the EI

Kernels	Emphysema index (%)				p-Value
	Mean	S.D.	Minimum	Maximum	
FC 10	55.4	12.6	17.2	77.1	<0.001
FC 12	54.0	12.9	15.3	76.6	–
FC 51	54.8	13.1	14.4	77.2	0.01
FC 85	59.9	11.5	23.4	78.6	<0.001

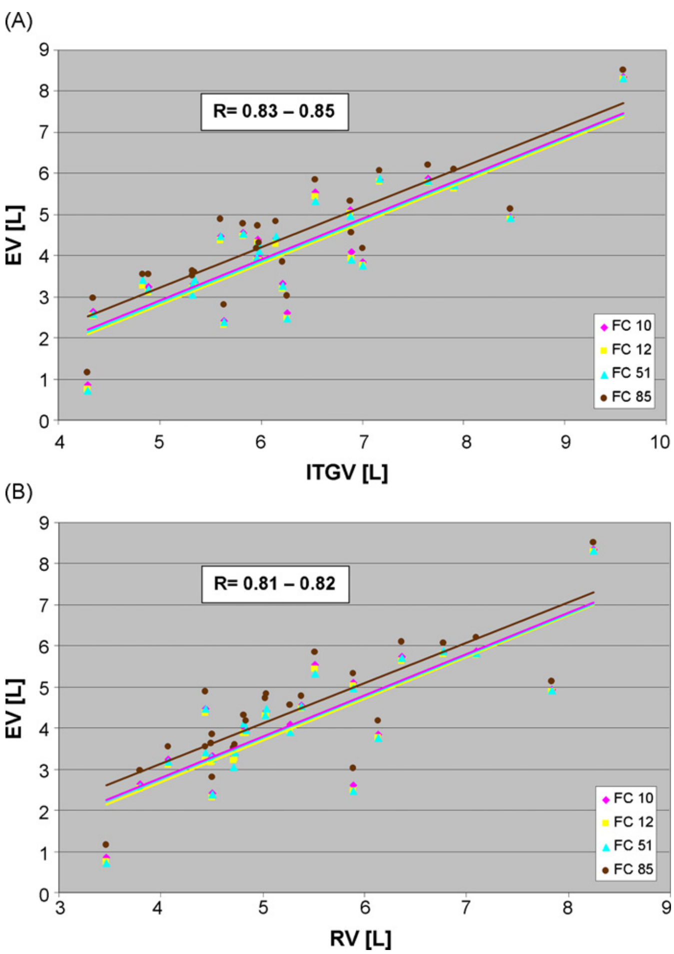

Fig. 5. Linear correlation between the emphysema volume (EV) and intra thoracic gas volume (ITGV) (A) and residual volume (RV) (B) as determined by pulmonary function test (PFT). The correlation coefficients for different reconstruction kernels revealed strong linear correlations between CT parameters and PFT results.

(Fig. 5). Moderate linear correlations ($R = 0.52–0.55$) were found between the EI and TLCO% predicted for all kernels (Table 4).

4. Discussion

In this study, the influence of different image reconstruction kernels on quantitative and volumetric image evaluation was performed for thoracic applications. Phantom measurements and patients with emphysema were investigated. EI, as a sensitive parameter for noise, showed no significant difference for all kernels without BHC. However, kernel FC 51 required a gaussian denoising filter. The use of BHC led to a significant decrease in MLD (5%) and EI (61–79%).

Table 4
This table shows the linear correlation coefficients between the CT evaluation for different kernels and pulmonary function tests

Kernels	Linear correlation (R)			
	LV vs. TLC	EV vs. ITGV	EV vs. RV	EI vs. TL_{CO} (%) predicted
FC 10	0.86	0.84	0.81	0.53
FC 12	0.86	0.84	0.82	0.54
FC 51	0.86	0.83	0.81	0.55
FC 85	0.86	0.85	0.82	0.52

Lung volume (LV); emphysema volume (EV); emphysema index (EI); total lung capacity (TLC); intrathoracic gas volume (ITGV); residual volume (RV); carbon monoxide transfer factor (TL_{CO}).

Beam collimation, X-ray tube voltage and tube current as well as the detector design determine the intrinsic resolution and quantum noise of a CT data set. These parameters cannot be changed retrospectively. Based on the intrinsic resolution and quantum noise of the data, image sharpness and pixel noise are modified in the image reconstruction process, mainly by the choice of different convolution kernels [25]. With the advent of MDCT, thorax examinations are routinely performed with thin-collimation (1 mm). These datasets are used as input for volumetric visualization, evaluation, and quantification of whole lung volume, emphysema volume, and emphysema index. This is of particular clinical importance as these quantitative parameters should be used in follow-up controls.

For visual analysis of chest CT images a high frequency reconstruction kernel (FC 51) is used. The high level of image noise is acceptable to the human eye as the evaluation benefits from the sharp contours of the septa [26].

Beam hardening correction was initially developed for imaging of the temporal bone and skull base. The efficacy of removing artefacts due to beam hardening in CT of the brain was demonstrated on a realistic, mathematically described phantom [16,27]. CT images of the chest sometimes show beam hardening artefacts in the posterior parts adjacent to the vertebral bodies. Thus, BHC intended to improve image quality in the paravertebral region. In a phantom, the modulation transfer function (MTF) curves for the BHC kernels showed no difference to the non-BHC kernels (Fig. 6) [28]. This was confirmed in our phantom measurements, where datasets reconstructed with BHC (FC 03 and FC 69) showed no significant difference to the kernels without BHC.

As the amount of beam hardening is determined dynamically based on the individual raw data, we assumed that BHC would not affect the whole lung parenchyma and the error introduced is kept to a minimum. However, the quantitative measurements in the lung parenchyma demonstrated a significant change of all parameters using BHC. Therefore, the use of any dynamically adapted changes of CT values should be avoided for quantitative evaluation of the lung parenchyma.

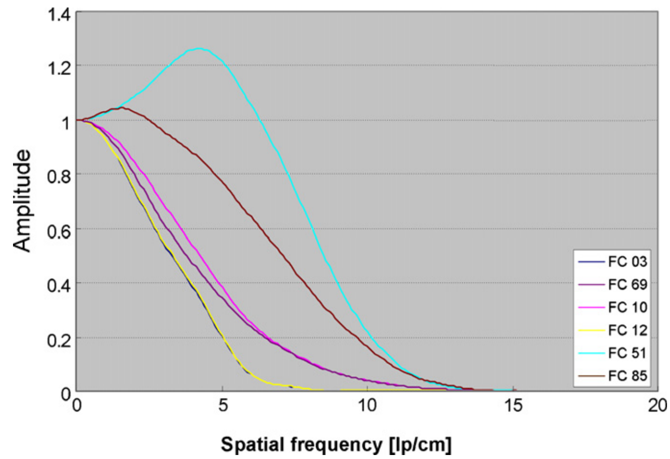

Fig. 6. Modulation transfer function (MTF) for the different kernels used in this study. As FC 51 shows a markely higher MTF quantitative analysis of images was only possible after an application of a denoising filter. This filter was not necessary for FC 85. In the chart there is no difference visible for kernels using beam hardening correction (BHC) like FC 03 and FC 69 and those without BHC (like FC 12 and FC 10).

For automatic segmentation of MDCT datasets, smooth kernels showed better results compared to high-resolution kernels as the image noise is substantially lower [22]. However, the effect of different reconstruction algorithms on quantitative evaluation of lung parenchyma and pathology in 3D was not shown yet. Some investigations were performed using three single slices or only 10 mm thick slices throughout the lung which do not allow for investigation of the fine structure of the lung parenchyma [13,29]. These image acquisition techniques are not sufficient as only thin slices (1.5 mm) showed a high correlation with pathologic specimens [30].

EI, for the most important parameter in emphysema, all kernels showed significant differences. However, the absolute differences were small 0.8–5.1%. As there is only a small variation of the emphysematous regions (range of $1 \pm 3\%$) in patients between two follow-up examinations, even small differences introduced by the reconstruction algorithm may lead to false positive or negative reports [31]. This underlines the necessity to use the same reconstruction algorithm for quantitative follow-up examinations.

Comparison with PFT indicates that a 3D-HRCT approach is superior to the old-fashioned single slice approach. While we found strong linear correlations between LV and EV with TLC, ITGV, and RV (0.81–0.86), in studies using a single slice approach correlation coefficients of 0.54 were found [7]. This may be explained mainly due to the inhomogeneous nature of emphysema. Assessing only some parts of the lung will not reflect the broad range of parenchymal changes. This is also seen in our patient population with the lowest EI of 15% and the highest EI of 77% (for FC 12).

The use of different reconstruction algorithms has merely any effect on the correlation with PFT.

As limitation it has to be mentioned that this study did not include comparison between different CT scanner vendors, which would have been of high interest. However, up to now it is not possible to perform reconstructions of “foreign” raw-data on different CT scanners.

5. Conclusion

A significant impact of the reconstruction algorithm on quantitative CT evaluation was found. Except for kernels with BHC, the absolute differences between different kernels were small, but they were larger than the known interscan variation in patients. Although significant differences were present for the quantitative parameters, no difference was found for the correlation with the functional parameters derived from PFT.

Therefore, for follow-up examinations it is essential to use the same reconstruction kernel to allow comparison between the datasets. It is of minor importance what specific kernel is chosen, as the correlation with PFT showed no difference.

References

[1] Bankier AA, Madani A, Gevenois PA. CT quantification of pulmonary emphysema: assessment of lung structure and function. Crit Rev Comput Tomogr 2002;43:399–417.

[2] Goldin JG. Quantitative CT of the lung. Radiol Clin North Am 2002;40: 145–62.

[3] Nakano Y, Muro S, Sakai H, et al. Computed tomographic measurements of airway dimensions and emphysema in smokers Correlation with lung function. Am J Respir Crit Care Med 2000;162:1102–8.

[4] Sakai N, Mishima M, Nishimura K, et al. An automated method to assess the distribution of low attenuation areas on chest CT scans in chronic pulmonary emphysema patients. Chest 1994;106:1319–25.

[5] Gould GA, MacNee W, McLean A, et al. CT measurements of lung density in life can quantitate distal airspace enlargement—an essential defining feature of human emphysema. Am Rev Respir Dis 1988;137:380–92.

[6] Madani A, Zanen J, de Maertelaer V, et al. Pulmonary emphysema: objective quantification at multi-detector row CT—comparison with macroscopic and microscopic morphometry. Radiology 2006;238:1036–43.

[7] Cerveri I, Dore R, Corsico A, et al. Assessment of emphysema in COPD: a functional and radiologic study. Chest 2004;125:1714–8.

[8] Cantor JO, Cerreta JM, Ochoa M, et al. Aerosolized hyaluronan limits airspace enlargement in a mouse model of cigarette smoke-induced pulmonary emphysema. Exp Lung Res 2005;31:417–30.

[9] Kurashima K, Takayanagi N, Sato N, et al. High resolution CT and bronchial reversibility test for diagnosing COPD. Respirology 2005;10:316–22.

[10] Uppaluri R, Mitsa T, Sonka M, et al. Quantification of pulmonary emphysema from lung computed tomography images. Am J Respir Crit Care Med 1997;156:248–54.

[11] Zaporozhan J, Ley S, Eberhardt R, et al. Paired inspiratory/expiratory volumetric thin-slice CT scan for emphysema analysis: comparison of different quantitative evaluations and pulmonary function test. Chest 2005;128:3212–20.

[12] Gevenois PA, Yernault JC. Can computed tomography quantify pulmonary emphysema? Eur Respir J 1995;8:843–8.

[13] Boedeker KL, McNitt-Gray MF, Rogers SR, et al. Emphysema: effect of reconstruction algorithm on CT imaging measures. Radiology 2004;232:295–301.

[14] Gevenois PA, de Maertelaer V, De Vuyst P, et al. Comparison of computed density and macroscopic morphometry in pulmonary emphysema. Am J Respir Crit Care Med 1995;152:653–7.

[15] Gevenois PA, De Vuyst P, de Maertelaer V, et al. Comparison of computed density and microscopic morphometry in pulmonary emphysema. Am J Respir Crit Care Med 1996;154:187–92.

[16] Herman GT. Demonstration of beam hardening correction in computed tomography of the head. J Comput Assist Tomogr 1979;3:373–8.

[17] McKenna Jr RJ, Gelb A, Brenner M. Lung volume reduction surgery for chronic obstructive pulmonary disease: where do we stand? World J Surg 2001;25:231–7.
[18] Toma TP, Hopkinson NS, Hillier J, et al. Bronchoscopic volume reduction with valve implants in patients with severe emphysema. Lancet 2003;361:931–3.
[19] Yim AP, Hwong TM, Lee TW, et al. Early results of endoscopic lung volume reduction for emphysema. J Thorac Cardiovasc Surg 2004;127:1564–73.
[20] Siafakas NM, Vermeire P, Pride NB, et al. Optimal assessment and management of chronic obstructive pulmonary disease (COPD). The European respiratory society task force. Eur Respir J 1995;8:1398–420.
[21] Blechschmidt RA, Werthschutzky R, Lorcher U. Automated CT image evaluation of the lung: a morphology-based concept. IEEE Trans Med Imaging 2001;20:434–42.
[22] Mayer D, Bartz D, Fischer J, et al. Hybrid segmentation and virtual bronchoscopy based on CT images. Acad Radiol 2004;11:551–65.
[23] Achenbach T, Weinheimer O, Buschsieweke C, et al. Fully automatic detection and quantification of emphysema on thin section MD-CT of the chest by a new and dedicated software. Fortschr Röntgenstr 2004;176:1409–15.
[24] Baldi S, Miniati M, Bellina CR, et al. Relationship between extent of pulmonary emphysema by high-resolution computed tomography and lung elastic recoil in patients with chronic obstructive pulmonary disease. Am J Respir Crit Care Med 2001;164:585–9.
[25] Schaller S, Wildberger JE, Raupach R, et al. Spatial domain filtering for fast modification of the tradeoff between image sharpness and pixel noise in computed tomography. IEEE Trans Med Imaging 2003;22: 846–53.
[26] Swensen SJ, Aughenbaugh GL, Brown LR. High-resolution computed tomography of the lung. Mayo Clin Proc 1989;64:1284–94.
[27] Herman GT. Correction for beam hardening in computed tomography. Phys Med Biol 1979;24:81–106.
[28] Droege RT, Morin RL. A practical method to measure the MTF of CT scanners. Med Phys 1982;9:758–60.
[29] Kemerink GJ, Lamers RJ, Pellis BJ, et al. On segmentation of lung parenchyma in quantitative computed tomography of the lung. Med Phys 1998;25:2432–9.
[30] Miller RR, Muller NL, Vedal S, et al. Limitations of computed tomography in the assessment of emphysema. Am Rev Respir Dis 1989;139:980–3.
[31] Stolk J, Dirksen A, van der Lugt AA, et al. Repeatability of lung density measurements with low-dose computed tomography in subjects with alpha-1-antitrypsin deficiency-associated emphysema. Invest Radiol 2001;36:648–51.